Journal of Neuroscience Research 76:481–487 (2004)

Dependence of Calcium Influx in Neocortical Cells on Temporal Structure of Depolarization, Number of Spikes, and Blockade of NMDA Receptors

Pavel Balaban,[1] Marina Chistiakova,[1,2] Aleksey Malyshev,[1] and Maxim Volgushev[1,2]★
[1]Institute of Higher Nervous Activity and Neurophysiology RAS, Moscow, Russia
[2]Department of Neurophysiology, Ruhr-University Bochum, Bochum, Germany

Increase of intracellular [Ca^{2+}] evoked by action potentials in a cell can induce long-term synaptic plasticity even without concomitant presynaptic stimulation. We used optical recording of the fluorescence of a Ca^{2+}-indicator Oregon Green to investigate whether differences in results obtained with modifications of that purely postsynaptic induction protocol could be due to differential Ca^{2+} influx. We compared changes of the somatic [Ca^{2+}] in layer II–III pyramidal cells in slices of rat visual cortex evoked by bursts of depolarization pulses and long depolarizing steps. During weak depolarizations, the Ca^{2+} influx was proportional to the amplitude and duration of the depolarization. With suprathreshold depolarizations, the Ca^{2+} influx was proportional to the number of action potentials. Because the burst depolarizations evoked more spikes than did the long duration steps, this burst protocol led to a larger Ca^{2+} influx. With all stimulation protocols, the spike-induced Ca^{2+} influx was reduced during blockade of *N*-methyl-D-aspartate (NMDA) receptors. Differences in intracellular [Ca^{2+}] increases thus may be one reason for differential effects of purely postsynaptic challenges on synaptic transmission.

Key words: rat; visual cortex; slices; calcium; Ca^{2+} imaging; intracellular tetanization

Induction of long-term plasticity in nerve cells critically depends on a coincidence between activation of synaptic receptors and a rise of intracellular calcium concentration (Bliss and Collingridge, 1993). Although substantial calcium influx occurs in dendrites and dendritic spines during synaptic stimulation in vitro (Müller and Connor, 1991; Miyakawa et al., 1992; Malinow et al., 1994; Markram and Sakmann, 1994; Petrozzino et al., 1995) and in vivo (Svoboda et al., 1997), generation of action potentials and an increased calcium concentration in the soma contribute significantly to induction of synaptic plasticity. This could be because action potentials that are generated at the soma may back-propagate in the dendritic tree and enhance local calcium influx at synapses (Larkum et al., 1999; Stuart and Häusser, 2001), or because the increase in calcium concentration influences biochemical machinery in the soma itself. The role of soma activation in plasticity induction is illustrated by two complementary lines of evidence. First, prevention of spiking and thus of the related somatic calcium influx by hyperpolarization effectively arrests induction of long-term potentiation (Kelso et al., 1986; Malinow and Miller, 1986). Second, the increase of intracellular [Ca^{2+}], evoked with bursts of short depolarization pulses (Kuhnt et al., 1994; Volgushev et al., 1994, 2000) or photolytically (Neveu and Zucker, 1996), can induce long-term changes of synaptic transmission in hippocampus and neocortex even without concomitant presynaptic stimulation. Interestingly, the effect of the depolarization-evoked [Ca^{2+}] increase on synaptic transmission depends on subtle modifications of that purely postsynaptic induction protocol. For example, in contrast to the long-lasting effect of bursts of short pulses, application of long depolarizations can lead to long-term changes (Alonso et al., 1990), short-term changes (Kullmann et al., 1992; Huang and Malenka, 1993), or no changes at all (Otsu et al., 1995). Further, our recent data show that blockade of the *N*-methyl-D-aspartate (NMDA) receptor prevents induction of long-term depression, but not long-term potentiation, by intracellular tetanization (Chistiakova et al., 1999). Understanding the reasons why such modifications of the induction protocol have different effects on synaptic transmission may help to clarify the mechanisms by which postsynaptic depolarization alone can induce long-term

Contract grant sponsor: Deutsche Forschungsgemeinschaft; Contract grant number: SFB 509 TP A5; Contract grant sponsor: NATO; Contract grant number: LST.CLG.978859.

★Correspondence to: M. Volgushev, Department of Neurophysiology, Ruhr-University Bochum, MA 4/149, D-44780 Bochum, Germany.
E-mail: maxim@neurop.ruhr-uni-bochum.de

Received 21 October 2003; Revised 10 February 2004; Accepted 12 February 2004

Published online 12 April 2004 in Wiley InterScience (www.interscience.wiley.com). DOI: 10.1002/jnr.20104

synaptic changes. One possible reason could be that these modifications of the induction protocol lead to differential Ca^{2+} influx. To address this question, we measured changes in somatic [Ca^{2+}] evoked by bursts of depolarization pulses and by long steps of different amplitudes of depolarization, both in control medium and during blockade of NMDA receptors. The Ca^{2+} influx was measured using optical recording of the fluorescence of Oregon Green, a calcium-sensitive dye.

MATERIALS AND METHODS

Slices (350 μm) of the visual cortex of 3–6-week-old rats were prepared by conventional methods as described previously (Volgushev et al., 2000) and investigated under submerged conditions at 32–34°C. Perfusion medium contained (in mM): 125 NaCl; 2.5 KCl; 2 $CaCl_2$; 1.25 NaH_2PO_4; 25 $NaHCO_3$; 1.5 $MgCl_2$; 25 D-glucose; and 0.5 L-glutamine bubbled with 95% O_2 and 5% CO_2. Recordings from pyramidal cells in layer II–III of the visual cortex were carried out with patch electrodes, containing (in mM): 127 K-gluconate; 20 KCl; 2 $MgCl_2$; 2 Na_2ATP; 10 HEPES; and 0.025 of fluorescent calcium-sensitive dye Oregon Green 488 BAPTA-1 (Molecular Probes, Eugene, OR; BAPTA is Ethylenedioxybis-(o-phenylenenitrilo)tetraacetic acid). The dye was first dissolved in the intracellular solution with addition of 1:1,000 of 20% Pluronic F127 in dimethylsulfoxide (DMSO) to a concentration of 0.15 mM and aliquots were stored frozen. For an experiment, an aliquot was diluted further 1:5 with the intracellular solution, so that the final concentration of the dye was 0.025 mM.

Intracellular recordings were made with an Axoclamp 2A amplifier and fed into a computer (PC-486, Digidata-1200, PClamp software; Axon Instruments). Intracellular stimulation was delivered either as a constant 400-msec step or a train of 20 pulses of 10-msec duration applied at 50 Hz, with a total burst duration of 400 msec. The amplitude of the stimulation current (or of the holding potential step in voltage clamp experiments) was varied from the subthreshold level for spike generation to an intensity at which spikes were evoked by each short pulse. Burst and step stimuli were delivered to the recorded cell in alternation with an intertrial interval of 1.5–2 min. In some later experiments with APV (d-(-)-2-Amino-5-phosphonopentanoic acid), we used only one or two different stimulus intensities throughout the experiment.

Recording of Ca^{2+} fluorescence was started 20–30 min after rupturing the membrane to let the dye penetrate the cell. For imaging, a CCD camera (SenSys1400; Photometrics, Tucson, AZ) was used. Acquisition of imaging data, its synchronization to intracellular stimulation, and recording of electrophysiologic data was carried out using MetaMorph software (Universal Imaging Corporation, Downingtown, PA). Intracellular Ca^{2+} changes are relatively slow; therefore, measurements of the Ca^{2+}-dependent fluorescence were carried out with 500 msec exposure per frame. The timing of the stimulation protocol is illustrated in Figure 1. The first frame (control) was acquired before the stimulus, the second one was synchronized with the beginning of the 400-msec stimulus (Fig. 1C; c2 and c3), and the third one with a 500-msec interval after the second frame. Fluorescence changes of Oregon Green were measured with single wavelength excitation (470 ± 20 nm) and emission (>510 nm). Changes in Ca^{2+} concentration changes are expressed as $\Delta F/F$, where F is the fluorescence intensity when the cell was at rest, and ΔF is the change in fluorescence during stimulation. Fluorescence intensity was measured in a region that covered a part of the soma. The region for measurements was located at the side of the soma opposite to the recording electrode and excluded the central, nucleus area. No corrections for indicator bleaching were made.

For statistical analysis of the data, *t*-test, Mann-Whitney test, and analysis of variance (ANOVA) were used. Differences were considered as significant if $P < 0.05$, unless otherwise specified.

RESULTS

We have measured changes of the Oregon Green fluorescence in response to long, 400-msec depolarization steps and bursts of short, 10-msec pulses of varying amplitude in 29 layer II–III pyramidal cells in rat visual cortex (Fig. 1). To achieve better control over the amplitude of membrane depolarization, we carried out the experiments in a voltage-clamp mode. In all 29 cells, increase of the fluorescence of the Ca^{2+} indicator was observed in response to suprathreshold stimulation, which led to generation of spikes. To access the time course of the fluorescence change in response to stimulation, as well as possible bleaching of the dye, we first recorded series of 10 frames (Fig. 1C, c1), with the stimulus applied synchronously with the beginning of the fourth frame (Fig. 1C, c3). Suprathreshold stimulation led to prolonged increase of the Ca^{2+} fluorescence, which was maximal during the stimulus and decreased slowly within 4–5 sec thereafter (Fig. 1C). Based on these results, we set the following main protocol for further experiments. The main protocol consisted of acquisition of three frames with 500-msec exposure time per frame, the stimulus been synchronized with the beginning of the second frame (Fig. 1c, c2). Because of the stable fluorescence intensity in the frames taken before the stimulus (frames 1–3 in Fig. 1C), there was no need to compensate the evoked fluorescence change for bleaching. In our main protocol, therefore, we acquired only one control frame before the stimulus. A 500-msec exposure time per frame allowed us to capture reliably the peak in fluorescence increase in the second frame. The third frame was taken to control for possible prolonged plateau responses at high intensity stimulation. At any stimulus intensity used in this study, however, the fluorescence increase in the third frame was always smaller than that in the second frame. For this reason, in further calculations of the Ca^{2+} response we used peak fluorescence increase, measured in the second frame. Figure 1D shows a typical example of fluorescence before stimulation (first frame, control), and its change during the stimulus (frames labeled stimulation, difference, and fluorescence change).

In 19 cells, we have measured the fluorescence of Ca^{2+} indicator during subthreshold stimulation, which did not lead to generation of spikes. In most of these cells (15 of 19), a clear increase in fluorescence was observed even when the amplitude of the holding potential step was

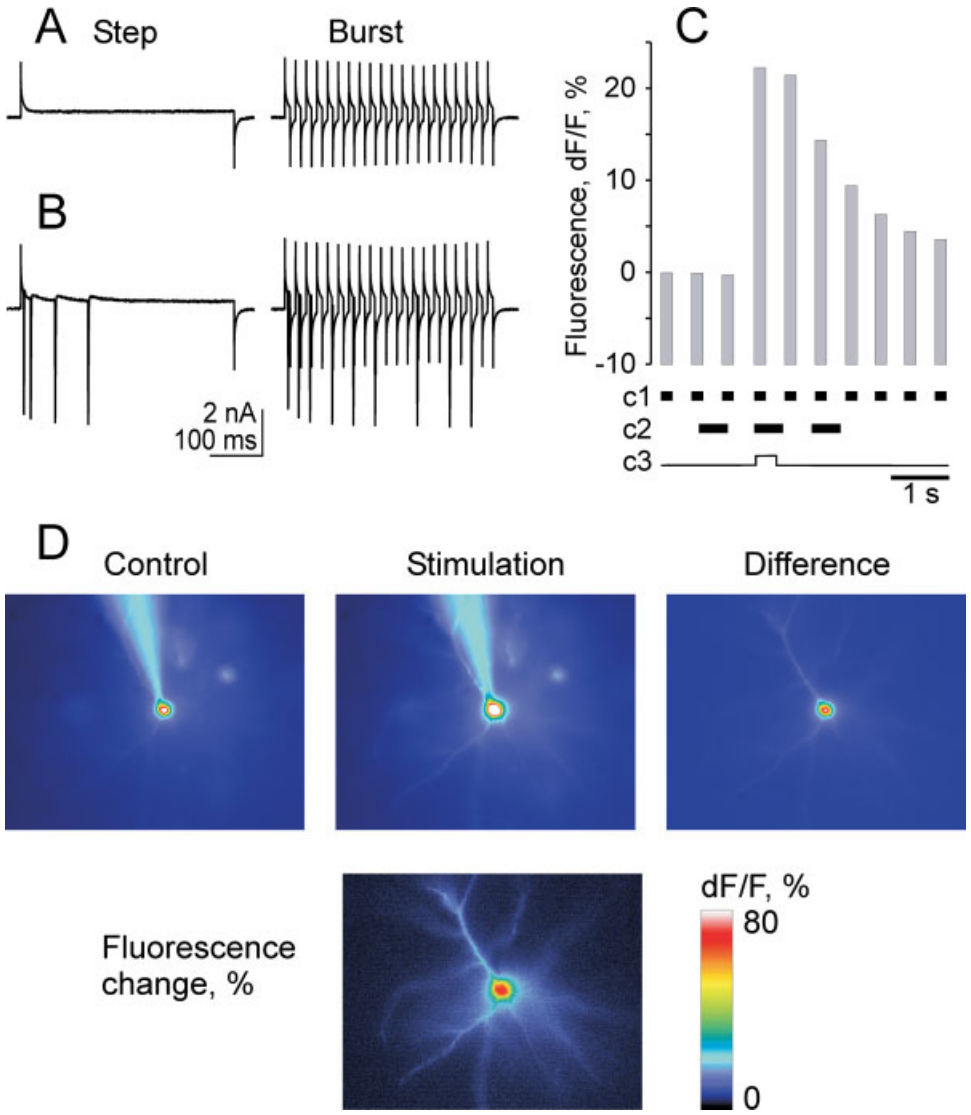

Fig. 1. Responses of layer II–III pyramidal cells to intracellular stimulation. **A, B:** Currents recorded in a voltage-clamped cell in response to a 400-msec constant step (left traces) or a burst of 20 pulses of 10-msec duration given at 50 Hz (right traces). Step amplitude was 30 mV (A) and 34 mV (B) from the holding potential of −80 mV. **C:** Changes in fluorescence of the calcium indicator Oregon Green 488 BAPTA-1 evoked by depolarization-induced spiking of a cell. Grey bars (top) show changes of the fluorescence of a cell relative to the background level measured in a series before (frames 1–3) and after the stimulation (frames 4–10). Frames were taken with 200-msec exposure, their timing is shown in c1. Intracellular depolarization pulse was synchronized with the beginning of the frame 4, as indicated in c3. Note that almost no bleaching occurred before the stimulation (frames 1–3). Timing of our main experiments is shown in c2 with exposure time of 500 msec/frame and the intracellular depolarization synchronized with the beginning of the second frame. Note that the frame 2 covers the peak of the fluorescence change. **D:** Images of a cell filled with Oregon Green 488 BAPTA-1, taken before (control) and during stimulation with a burst of suprathreshold pulses. The rightmost image shows the difference between the stimulation and control frames. The lowermost image, showing fluorescence change, was obtained by dividing the frame Difference by the frame Control. The pseudocolor scale belongs to the fluorescence change frame only.

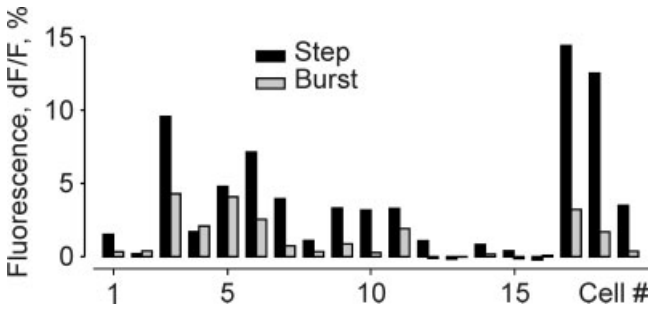

Fig. 2. Change of Oregon Green fluorescence in 19 layer II–III pyramidal cells in response to a long step (400 ms, black bars) or a burst (20 pulses, 10-msec duration at 50 Hz, grey bars) of a just-subthreshold strength. For each cell, the amplitude for the long step and the pulses in a burst was the same.

below the threshold for spike activation. In Figure 2, data obtained at intensities just subthreshold for spike activation are shown for the 19 cells. Despite considerable variability of the amplitude of the fluorescence change among the cells, stronger Ca^{2+} influx was produced consistently by long steps compared to that by bursts of short steps (Fig. 2). On average, the fluorescence change during the burst was $1.2 \pm 0.3\%$ compared to $3.8 \pm 0.9\%$ ($n = 19$, $t = 3.3$, $P < 0.01$) during the long step of the same amplitude. During low amplitude depolarizations, therefore, the influence of total depolarization duration, which was 400 msec during the long pulse, but only 200 msec during the burst, overcompensates for possible effects of voltage-gated calcium channel inactivation.

With stimuli of stronger intensity that led to spike generation (Fig. 1B), the relation was reversed. The increase of intracellular [Ca^{2+}] was larger during stimulation with bursts compared to that with long pulses (Fig. 3A

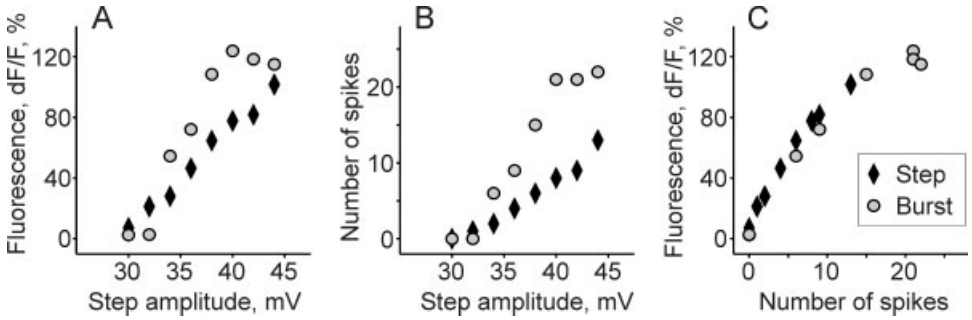

Fig. 3. Relation between Oregon Green fluorescence changes, amplitude of the membrane potential step, and the number of spikes in a layer II pyramidal cell. **A:** Dependence of the fluorescence change on the amplitude of the holding potential step. **B:** Dependence of number of spikes on the amplitude of the holding potential step. **C:** Dependence of the fluorescence change on the number of spikes.

exemplifies this relation). In the plot of fluorescence change against step amplitude of the holding potential, burst stimuli consistently led to larger changes of the fluorescence than did long pulses of the same amplitude (Fig. 3A). This inversion of the relation between the Ca^{2+} influx, produced by bursts and long pulses, was due to the fact that more spikes were evoked by bursts of short depolarizations than by long pulses (Fig. 3B). Apparent saturation of the fluorescence increase in response to burst stimulation corresponded to saturation of the number of spikes evoked by the burst (about one spike per short pulse) (Fig. 3A,B). The lowered efficacy of long depolarizations in generation of spikes has been described elsewhere (Mainen and Sejnowski, 1995; Nowak et al., 1997; Volgushev et al., 1998) and was attributed to spike adaptation and inactivation of the voltage-gated sodium channels. To separate the influence of the number of spikes from that of stimulus shape on Ca^{2+} influx, we plotted the fluorescence change against the spike number for both kinds of stimuli. The plot in Figure 3C shows an almost identical dependence of the fluorescence change on spike number, with little difference between step- or burst-evoked spikes. The relationships between step amplitude, fluorescence changes, and spike number in responses (Figure 3) were typical for cells in our sample. Similar results were observed in eight neurons in which both bursts and long steps of at least five different amplitudes were applied, which allowed to build the dependence of the fluorescence change on the depolarization amplitude and the number of spikes in response.

In the cell shown in Figure 3, as well as in other cells, dependence of the fluorescence change on spike number in response was almost linear until less than 10 spikes were generated. At high stimulus intensities, when there was more than about 10–15 generated spikes, the amplitude of the evoked fluorescence change showed a tendency for saturation (Fig. 3C). To quantify the saturation, we segregated the data for each cell into two groups; one group comprised responses with less than 10 spikes and the other group, responses with more than 10 spikes. For each response in both groups, we divided the measured fluorescence change by the number of spikes, thus calculating the fluorescence increase per spike. The fluorescence increase per spike was significantly less during stronger than during weaker responses (Fig. 4A). When evoked with long steps, each spike led to a fluorescence increase of $8.84 \pm 1.37\%$ per generated spike during weaker responses, but to only $4.9 \pm 0.58\%$ during stronger responses ($P < 0.01$, ANOVA, $n = 13$). Significantly higher increase of the fluorescence per spike was also observed during weaker than during stronger responses evoked by bursts ($7.7 \pm 1.21\%$ vs. $3.9 \pm 0.39\%$, $P < 0.01$, $n = 13$). The contribution of each spike is significantly less for both pulse and burst stimuli in the group of stronger (>10 spikes) than in the group of weaker (<10 spikes) responses. Two possible reasons might account for saturation of the Ca^{2+} influx magnitude during strong stimulation. First, it could be due to saturation of the dye. This is very unlikely, because the same relationship that indicates a smaller contribution per spike in the case of stronger responses was observed in the experiments with APV (see below, Fig. 4), when all fluorescence changes were of a lower amplitude. One further argument against dye saturation comes from experiments with different stimulus duration. In these experiments, we measured the time for saturation of Ca^{2+}-induced increase of fluorescence using stimuli of longer duration. Five frames, each one with 500-msec exposure, were acquired after the stimulus. It was found that the total response stopped increasing when the stimulus was significantly longer (in the range of 3–5 sec) than was the one (0.4 sec) we have used in the main experiments (data not shown). These data show that in our main experiments the dye was not saturated and the upper limit of the total possible Ca^{2+} influx was not reached. The second, more realistic possibility is inactivation of the voltage-dependent calcium channels during strong depolarizations eliciting Ca^{2+} influx. Within both groups (>10 and <10 spikes), no significant difference was found between the fluorescence change per spike elicited by long steps or bursts (Fig. 4A, black columns).

We have demonstrated recently (Chistiakova et al., 1999) that blockade of the NMDA-receptors in rat visual

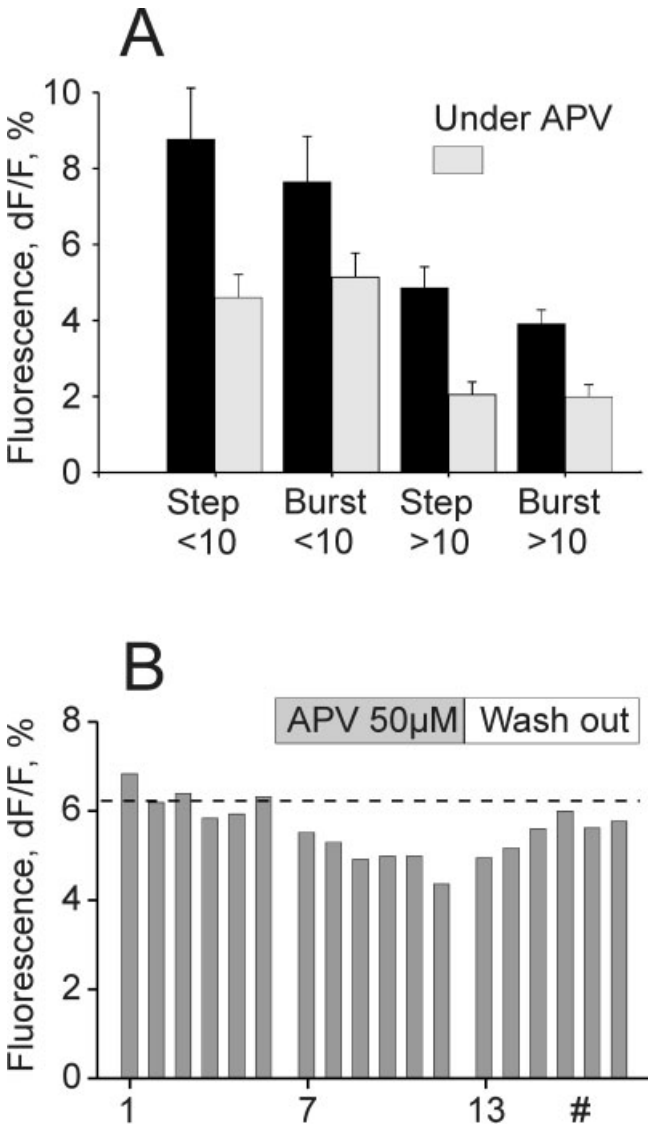

Fig. 4. Blockade of the NMDA receptors reversibly reduces depolarization-induced Ca^{2+} influx in layer II–III pyramidal cells. **A:** Comparison of fluorescence change in response to a long step and a burst of short pulses, recorded in a control medium (black bars) and after addition of 0.05 mM APV (grey bars). Averaged data from 13 layer II–III pyramidal cells corrected for number of spikes. In all four groups, Ca^{2+} influx was reduced significantly under APV. $P < 0.05$ for bursts eliciting less than 10 spikes, $P < 0.01$ for three other groups. **B:** Reversibility of Ca^{2+} influx reduction by APV in a layer II pyramidal cell. Time course of fluorescence change in response to a depolarization step corrected for number of spikes. Measurements were made every 3 min. APV was added to the recording medium between measurements 6 and 7, and the washout started between measurements 12 and 13, as indicated. Note the reduction in fluorescence change during APV application and its recovery upon washout.

cortex prevents induction of long-term depression (LTD) of synaptic transmission by intracellular tetanization. To test whether blockade of NMDA receptors reduces Ca^{2+} influx induced by depolarization without synaptic stimulation, we measured the Ca^{2+} influx as described above in the control medium and after addition of 0.05 mM APV to the medium in 13 cells. NMDA receptor blockade with APV led to a significant reduction of the depolarization-induced Ca^{2+} influx. In the group of responses with less than 10 spikes, long depolarization pulses led to an increase in Ca^{2+} fluorescence of 8.84 ± 1.37% per generated spike in the control medium, but only to 4.64 ± 0.61% per spike in the medium with APV ($P < 0.01$, Fig. 4A, step <10). With bursts of short pulses, the Ca^{2+} fluorescence increased by 7.7 ± 1.21% per spike in the control, and by 5.18 ± 0.64% after APV application ($P < 0.05$, Fig. 4A, burst <10). The significant reduction of the Ca^{2+} influx into the cell in the presence of APV was not accompanied by a change in spike number of the responses. In the group of responses with less than 10 spikes, depolarization with long steps led to generation of 4.41 ± 0.67 spikes in control conditions and 4.6 ± 0.52 spikes after application of APV. With bursts of short depolarizations, the averaged number of spikes in response was 5.9 ± 0.78 before and 5.35 ± 0.72 after APV application. Similar relations were also found for the responses to stronger depolarizations, when more than 10 spikes were generated. Addition of APV to the recording medium significantly reduced Ca^{2+} influx without altering the averaged number of spikes in responses (Fig. 4). In all modes of stimulation, either weak or strong, with long pulses or bursts of short pulses, APV blockade of NMDA receptors thus led to a significant decrease of the Ca^{2+} fluorescence signal.

In an additional series of experiments, we have checked the reversibility of the reduction in Ca^{2+}-induced fluorescence by APV application in four cells. Results of a sample experiment are shown in Figure 4B, where each bar shows the amplitude of the fluorescence change induced by the stimuli of the same intensity. The response was reduced during the application of 0.05 mM APV, but recovered after the drug was washed out. Similar results were obtained in three other experiments with this protocol, indicating the reduction of the amplitude of the intracellular Ca^{2+} signal in the presence of APV was reversible.

DISCUSSION

Our measurements of the fluorescence of the calcium indicator Oregon Green show that, in accordance with previous reports (Miyakawa et al., 1992; Markram and Sakmann, 1994; Petrozzino et al., 1995), during low amplitude depolarizations that remain below the threshold for action potential generation, the Ca^{2+} influx depends primarily on amplitude and duration of depolarization. The impact of the inactivation of voltage-dependent calcium channels remains negligible during subthreshold stimulation. With stronger depolarizations, $[Ca^{2+}]$ increase is caused predominantly by action potentials and associated currents. The similarity of the dependence of the strength of the Ca^{2+} influx in response to long pulses and to bursts of short pulses on the number of spikes indicates, that also during strong depolarization there is no significant difference between the two stimulation proto-

cols with respect to the balance of inactivation and deinactivation of calcium channels. The larger increase of intracellular [Ca^{2+}] evoked by the burst depolarization as compared to the long depolarization steps of the same amplitude is due to the larger number of the spikes evoked by the burst.

We have demonstrated recently (Chistiakova et al., 1999) that induction of long-term depression (LTD) of synaptic transmission to layer II–III pyramidal cells in rat visual cortex by intracellular tetanization depends on activation of NMDA receptors and is abolished by their blockade. We have speculated that this unexpected finding could be explained by the presence of minor amounts of background glutamate in a slice, which could be bound to some NMDA receptors due to their extremely high affinity (Clements and Westbrook, 1991). This does not lead to a Ca^{2+} influx at rest, because NMDA receptor channels are blocked by magnesium (Nowak et al., 1984), but when the magnesium block is removed by intracellular tetanization, some Ca^{2+} enters the cell through open channels. To test this prediction, we measured the Ca^{2+} influx as described above in the control medium, and after addition of 0.05 mM APV to the medium. In all modes of stimulation, either weak or strong, with long pulses or bursts of short pulses, APV blockade of NMDA receptors led to a significant decrease of Ca^{2+} influx (Fig. 4). This effect of NMDA receptor blockade is unlikely to be due to alteration of network properties. Despite the high density of synapses at neocortical cells, connections between individual cells are weak (e.g., Thomson and West, 1993). Consequently, activation of a single cell cannot evoke action potentials in the postsynaptic targets and thus cannot cause substantial network activity. There is evidence that reduction of the calcium influx by APV might hold also for the excitatory postsynaptic potential (EPSP)-shaped depolarizations in dendrites of pyramidal cells. In a study of calcium transients in dendrites of neocortical pyramidal cells, Markram and Sakmann (1994) demonstrated that APV application markedly reduces calcium influx evoked by synaptic stimulation. Although they have not analyzed it quantitatively, a decrease of total calcium influx in response to a simulated EPSP-shaped depolarization under APV can be clearly seen in Figure 4 of Markram and Sakmann (1994). The reduction in Ca^{2+} influx evoked by depolarization in the presence of APV shows that under conditions when depolarization is evoked by synaptic stimulation, a certain amount of Ca^{2+} may enter the cell through the NMDA receptor-gated channels even at nonactivated synapses. Although the Ca^{2+} influx at the nonactivated sites is of a smaller magnitude than that at active synapses, these modest increases of intracellular [Ca^{2+}] may be important for induction of heterosynaptic plastic changes. Furthermore, these data support the notion that some background glutamate is present in the slice, and is sensed by the high-affinity NMDA receptors (Chistiakova et al., 1999).

Taken together, the results of our study show that even subtle modifications of the protocol of cell depolarization are associated with changes of the Ca^{2+} influx into the cell. The differences in intracellular [Ca^{2+}] increase may be one reason for the different effects of purely postsynaptic challenges on synaptic transmission (Alonso et al., 1990; Kullmann et al., 1992; Huang and Malenka, 1993; Kuhnt et al., 1994; Volgushev et al., 1994, 2000; Otsu et al., 1995; Neveu and Zucker, 1996; Chistiakova et al., 1999).

ACKNOWLEDGMENTS

We thank U. Eysel for support of this work, T. Vidyasagar for improving the English, and C. Tacke for excellent technical assistance.

REFERENCES

Alonso A, de Curtis M, Llinas, R. 1990. Postsynaptic Hebbian and non-Hebbian long-term potentiation of synaptic efficacy in the entorhinal cortex in slices and in the isolated adult guinea pig brain. Proc Natl Acad Sci USA 87:9280–9284.

Bliss TV, Collingridge GL. 1993. A synaptic model of memory: long-term potentiation in the hippocampus. Nature 361:31–39.

Chistiakova M, Balaban PM, Eysel UT, Volgushev M. 1999. NMDA receptor blockade prevents LTD, but not LTP induction by intracellular tetanization. Neuroreport 10:3869–3874.

Clements JD, Westbrook GL. 1991. Activation kinetics reveal the number of glutamate and glycine binding sites on the *N*-methyl-D-aspartate receptor. Neuron 7:605–613.

Huang YY, Malenka RC. 1993. Examination of TEA-induced synaptic enhancement in area CA1 of the hippocampus: the role of voltage-dependent Ca^{2+} channels in the induction of LTP. J Neurosci 13:568–576.

Kelso SR, Ganong AH, Brown TH. 1986. Hebbian synapses in hippocampus. Proc Natl Acad Sci USA 83:5326–5330.

Kuhnt U, Kleschevnikov AM, Voronin LL. 1994. Long-term enhancement of synaptic transmission in the hippocampus after tetanization of single neurones by short intracellular current pulses. Neurosci Res Comm 14:115–123.

Kullmann D, Perkel D, Manabe T, Nicoll R. 1992. Ca^{2+} entry via postsynaptic voltage-sensitive Ca^{2+} channels can transiently potentiate excitatory synaptic transmission in the hippocampus. Neuron 9:1175–1183.

Larkum ME, Zhu JJ, Sakmann B. 1999. A new cellular mechanism for coupling inputs arriving at different cortical layers. Nature 398:338–341.

Mainen ZF, Sejnowski TJ. 1995. Reliability of spike timing in neocortical neurons. Science 268:1503–1506.

Malinow R, Miller JP. 1986. Postsynaptic hyperpolarization during conditioning reversibly blocks induction of long-term potentiation. Nature 320:529–530.

Malinow R, Otmakhov N, Blum K, Lisman J. 1994. Visualizing hippocampal synaptic function by optical detection of Ca^{2+} entry through the *N*-methyl-D-aspartate channel. Proc Natl Acad Sci USA 91:8170–8174.

Markram H, Sakmann B. 1994. Calcium transients in dendrites of neocortical neurons evoked by single subthreshold excitatory postsynaptic potentials via low-voltage-activated calcium channels. Proc Natl Acad Sci USA 91:5207–5211.

Miyakawa H, Ross WH, Jaffe D, Callaway JC, Lasser-Ross N, Lisman JE, Johnston D. 1992. Synaptically activated increases in Ca^{2+} concentration in hippocampal CA1 pyramidal cells are primarily due to voltage-gated Ca^{2+} channels. Neuron 9:1163–1173.

Müller W, Connor JA. 1991. Dendritic spines as individual neuronal compartments for synaptic Ca^{2+} responses. Nature 354:73–76.

Neveu D, Zucker RS. 1996. Postsynaptic levels of [Ca^{2+}]i needed to trigger LTD and LTP. Neuron 16:619–629.

Nowak L, Bregestovski P, Ascher P, Herbet A, Prochiantz A. 1984. Magnesium gates glutamate-activated channels in mouse central neurones. Nature 307:462–465.

Nowak LG, Sanchez Vives MV, McCormick DA. 1997. Influence of low and high frequency inputs on spike timing in visual cortical neurons. Cereb Cortex 7:487–501.

Otsu Y, Kimura F, Tsumoto T. 1995. Hebbian induction of LTP in visual cortex: perforated patch-clamp study in cultured neurons. J Neurophysiol 74:2437–2444.

Petrozzino JJ, Pozzo Miller LD, Connor JA. 1995. Micromolar Ca^{2+} transients in dendritic spines of hippocampal pyramidal neurons in brain slice. Neuron 14:1223–1231.

Stuart GJ, Häusser M. 2001. Dendritic coincidence detection of EPSPs and action potentials. Nat Neurosci 4:63–71.

Svoboda K, Denk W, Kleinfeld D, Tank DW. 1997. In vivo dendritic calcium dynamics in neocortical pyramidal neurons. Nature 358:161–165.

Thomson AM, West DC. 1993. Fluctuations in pyramid-pyramid excitatory postsynaptic potentials modified by presynaptic firing pattern and postsynaptic membrane potential using paired intracellular recordings in rat neocortex. Neuroscience 54:329–346.

Volgushev M, Balaban P, Chistiakova M, Eysel UT. 1998. Involvement of two types of retrograde signalling in neocortical synaptic plasticity. Eur J Neurosci 10(Suppl):22.

Volgushev M, Balaban P, Chistiakova M, Eysel UT. 2000. Retrograde signalling with nitric oxide at neocortical synapses. Eur J Neurosci 12:4255–4267.

Volgushev M, Voronin LL, Chistiakova M, Singer W. 1994. Induction of LTP and LTD in visual cortex neurones by intracellular tetanization. Neuroreport 5:2069–2072.